An Integrated Platoon and UAV System for 3D Localization in Search and Rescue

Hongming Zhang*, Li Wang†*, and Aiguo Fei*
*School of Software Engineering, Beijing University of Posts and Telecommunications, Beijing, China
†School of Electronic Engineering, Beijing University of Posts and Telecommunications, Beijing 100876, China

***Abstract*—In search and rescue (SAR), survivals localization information is required to be obtained as quickly and accurately as possible. However, due to the accidental and destructive natural of emergency events, existing network infrastructures and devices may be unable to perform the localization tasks. Furthermore, survivals may be trapped in isolated areas, where human being is unable to reach. To address these issues, in this paper, we propose an integrated platoon and unmanned aerial vehicle (UAV) system for implementing the three-dimensional (3D) localization task in SAR, where the platoon is consisted of self-driving vehicles. Specifically, UAVs are controlled by these vehicles to perform the 3D localization task. Furthermore, in order to facilitate 3D localization, a platoon-aided UAV deployment strategy is proposed, where UAVs are deployed in different places for collecting direction-of-arrival (DoA) information of a target. As a further enhancement, a rotational invariance based beamforming (RIB) scheme is conceived to provide a simple DoA estimation for our multiple-in-multiple-out (MIMO) UAVs. Simulation results are provided for evaluating the system performance, showing that it is capable of achieving a beneficial trade-off between the attainable 3D localization performance and the corresponding time delay.**

***Index Terms*—search and rescue, 3D localization, unmanned aerial vehicle, platoon, wireless emergence communications, beamforming**

I. Introduction

Search and rescue (SAR) constitutes one of the most significant missions, is required to be conducted rapidly and efficiently. A compelling technique is to design an intelligent SAR system relying on advanced technologies, such as platooning control conceived for autonomous driving and unmanned aerial vehicle (UAV).

In vehicular platooning, a group of vehicles with common interests cooperatively form a platoon-based driving pattern, where a carefully controlled inter-vehicle distance is maintained [1]. With the aid of advanced wireless communication technologies, each vehicle in the platoon is capable of monitoring its vicinity, yielding a safe driving scenario [2], [3]. Moreover, it also has the advantage of increasing the road's traffic capacity, reducing fuel consumption, gas emissions, etc. Thus, such a platooning control aided self-driving system results in a reliable transportation system, which is also suitable for SAR missions and for delivering emergency supplies.

Furthermore, as a benefit of their agility and bird's-eye perspective, UAVs are capable of improving the support of SAR. Typically, UAVs can be classified into two categories, namely fixed-wing and rotary-wing UAVs [4]. Fixed-wing UAVs are capable of high-speed flight despite carrying heavy payloads in transportation applications. By contrast, rotary-wing UAVs with limited velocity and payload are more suitable for stationary applications in the absence of base station (BS) coverage [5].

As an important part of SAR, the position of a survivor (or of a target) has to be known. Here, since the computing and communication resources are limited in hostile environments, the localization is ideally by UAVs, given their excellent field of vision [6]–[12]. In [6], an experimental UAV platform was investigated both in indoor and outdoor environments, where localization information was gleaned from camera images. ultrawide bandwidth (UWB) localization was characterized in [7], showing that a decimeter-order localization accuracy was attainable. However, the UWB-based methods rely on expensive devices. By leveraging the Doppler effect of the targets' signals, a SAR system was proposed in [8], where a reduced rescue time was attained by the proposed system. In [9], a multi-UAV system was conceived to maximize the capacity by tackling a joint optimization problem of trajectory and power allocation. A direction-of-arrival (DoA) based self-positioning algorithm was designed in [10], while in [11], a deep reinforcement learning based approach was proposed for solving UAV navigation problems in a complex large-scale environment. As a further development, a sophisticated particle filter based algorithm was proposed in [12].

Against the above background, the novel contributions of this paper are summarized as follows:

- *We propose an integrated platooning and UAV system for solving localization problems in SAR. Moreover, a platooning-aided UAV deployment strategy is proposed for solving three-dimensional (3D) localization tasks based on DoA estimation performed by UAVs.*
- *Explicitly, a rotational invariance based beamforming (RIB) scheme is conceived for multiple-in-multiple-out (MIMO) UAV transceiver relying on a closed-formed function of the received signals as its inputs. The system performance is investigated by simulation results, demonstrating that our proposed system is capable of accurate 3D localization results in SAR.*

The rest of the paper is organized as follows. In Section II, the integrated platooning and UAV system is described. Then, our RIB design is detailed in Section III. In Section IV, we conceive our platooning-based UAV deployment strategy and

3D localization solutions, followed by our simulation results in Section V. Finally, we offer our conclusions in Section VI.

II. Integrated Platooning and UAV System for SAR

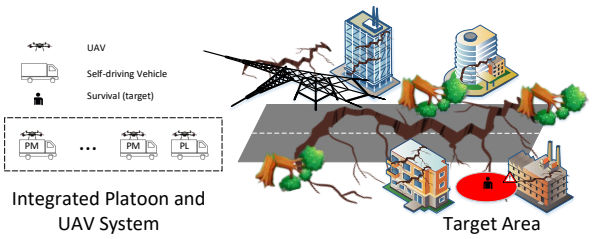

Fig. 1: Illustration of an integrated platooning and UAV system for SAR.

The proposed system is illustrated in Fig. 1, where a single platoon is considered. As shown in Fig. 1, the platoon consists of a platoon leader (PL) and $(V-1)$ platoon members (PMs), where the PL is responsible for platoon control and management, 3D localization, and so on. Specifically, in our proposed system, UAVs are carried by the self-driving vehicles in the platoon for estimating DoA of a target. On the other hand, a member vehicle, also known as (a.k.a.) the platoon member (PM), is a following vehicle of the PL. In our system, PMs are responsible for communicating with the PL as well as for controlling their UAVs, as it will be detailed in Section IV.

Generally, in order to maintain the platoon's stability, cooperative awareness messages (CAMs) are shared by the PL and PMs at each update cycle. In this paper, due to its distinct stability features, a predecessor-leader controller strategy [13] is assumed to be applied for disseminating CAMs among platoon vehicles. As seen in Fig. 1, SAR is assumed to be implemented by the integrated platoon and UAV system without the aid of other networks that can provide centralized management and control (i.e. the network infrastructure is not deployed in the target area or the network infrastructure is broken). In this paper, we focus our attention on the case of a single target that is trapped in an isolated location. As soon as the platoon arrives at the target area, a target localization task is executed by the PL. Before giving solutions to the target localization, let us introduce our RIB design for UAVs, as detailed in the next section.

III. Rotational Invariance based Beamforming Design for UAVs

In this section, our rotational invariance based beamforming design for the DoA estimation in UAVs is detailed. We commence by introducing the UAV-aided communications system. Then, the DoA estimation problem in our system is formulated. Finally, we propose the RIB design for UAVs.

A. MIMO UAV Modeling

Each UAV is assumed to be equipped with M transmit antennas (TAs) and N receive antennas (RAs), where we have $N \geq 2$ and $M \geq 2$. In particular, the M TAs are divided into L subarrays, where we have $L \leq M$. On the other hand, the target is assumed to be equipped with a single passive antenna. We assume that the angles of the target observed by the TA array and the RA array of a given UAV are almost the same, since the distance between the UAV and the target is much larger than the distance of the TA array and the RA array of the UAV. Let us denote this angle as θ. Furthermore, a uniform linear array (ULA) arrangement is assumed to be deployed by the UAV with a half-wavelength separation between two adjacent antennas. In this case, the transmit and receive steering vectors are given by [14] $\boldsymbol{a}(\theta) \triangleq [1, \exp(-j\pi\sin\theta), \ldots, \exp(-j\pi(M-1)\sin\theta)]^T$ and $\boldsymbol{b}(\theta) \triangleq [1, \exp(-j\pi\sin\theta), \ldots, \exp(-j\pi(N-1)\sin\theta)]^T$, respectively. Furthermore, we assume that $\boldsymbol{a}(\theta)$ and $\boldsymbol{b}(\theta)$ are known functions of θ by UAVs.

Firstly, a narrowband signal denoted as $u_l(t)$ is generated for the lth transmit subarray. Here, the baseband waveforms for different transmit elements are assumed to be orthogonal and have unit energy, i.e., we have

$$\int_0^{T_s} u_i(t)u_j^*(t)\mathrm{d}t = \begin{cases} 0 & \text{if } i \neq j, \\ 1 & \text{if } i = j, \end{cases} \tag{1}$$

where T_s denotes the symbol period. Then, the transmit beamforming matrix denoted as $\boldsymbol{W} \in \mathbb{C}^{M\times L}$ is applied to the L baseband waveforms, giving $\boldsymbol{W}\boldsymbol{u}(t)$, where $\boldsymbol{u}(t) = [u_0(t), \ldots, u_{L-1}(t)]^T$ is the baseband waveform vector. Next, the radio frequency (RF) interface of the UAV generates the continuous wave (CW), which is radiated towards the targeted area. Since a passive antenna is used, the target simply sends the received signal back to UAV without proceeding any further coding or signal processing process. Hence, the baseband equivalent observations at the UAV denoted as $\boldsymbol{y}(t) = [y_0(t), \ldots, y_{N-1}(t)]^T$ can be modeled as [14]

$$\boldsymbol{y}(t) = \rho\boldsymbol{a}^T(\theta)\boldsymbol{W}\boldsymbol{u}(t)\boldsymbol{b}(\theta) + \boldsymbol{n}(t), \tag{2}$$

where ρ is the attenuation coefficient of forward and backward path loss. In (2), $\boldsymbol{n}(t)$ contains background noise and interference, which can be modeled as circularly symmetric complex white Gaussian noise with zero-mean and a variance of N_0.

Upon applying matched filtering, the lth observation at the nth receive antenna of the UAV can be formulated as

$$y_{n,l} = \int_0^{T_s} y_n(t)u_l^*(t)\mathrm{d}t = \rho\boldsymbol{a}^T(\theta)\boldsymbol{w}_l b_n(\theta) + n_{n,l}, \tag{3}$$

where $\boldsymbol{w}_l$ denotes the lth column of the beamforming matrix $\boldsymbol{W}$. Based on (3), the conditional probability density function (PDF) can be expressed as

$$p(y_{n,l}|\rho,\theta) = \frac{1}{\pi N_0}\exp\left\{-\frac{\left|y_{n,l} - \rho\boldsymbol{a}^T(\theta)\boldsymbol{w}_l b_n(\theta)\right|^2}{N_0}\right\}, \tag{4}$$

for $n = 0, \ldots, N-1$ and $l = 0, \ldots, L-1$.

B. Problem Statement

We are interested in estimating the unknown parameter θ from the given observation vector denoted as $\boldsymbol{y} = [y_{0,0}, \ldots, y_{0,L-1}, \ldots, y_{N-1,0}, \ldots, y_{N-1,L-1}]^T$. Typically, the optimal estimator invokes the maximum *a posterior* (MAP) principle by solving the optimization problem of

$$\theta^{\text{opt}} = \arg\max_{\forall\theta} p(\theta|\boldsymbol{y}), \tag{5}$$

where $p(\theta|\boldsymbol{y})$ is the *a posteriori* probability of θ given $\boldsymbol{y}$. Assuming the probability $p(\theta)$ is equiprobable and independent. Then, the MAP estimator of (5) can be equivalent to

$$\theta^{\text{opt}} = \arg\max_{\forall\theta} \mathbb{E}_{\rho}\left[p(y_{n,l}|\rho,\theta)\right], \tag{6}$$

where the conditional PDF $p(y_{n,l}|\rho,\theta)$ is given in (4). Note that (6) can be solved via exhaustive search of all the possible values of ρ. However, the corresponding computational cost might become excessive in practice, especially for UAV and the PL, where the logic and memory resources are limited. Below, we propose a beamforming design to accomplish a low cost estimation of the unknown parameter θ.

C. Rotational Invariance based Beamforming Design

Firstly, we are interested in solving the problem of estimating the unknown parameter θ without leveraging any knowledge of ρ. A remedy to this issue is the rotational invariance technique, where θ can be estimated by exploiting the rotational invariance property (RIP) of the underlying signal subspace. To this end, the beamforming matrix $\boldsymbol{W}$ is required to be specifically designed, as shown below.

For the sake of demonstration, let us define the first term of (3) as

$$r_{n,l} \triangleq \rho \boldsymbol{a}^T(\theta)\boldsymbol{w}_l b_n(\theta) = \rho\Theta_l b_n(\theta), \tag{7}$$

where, by definition, we have

$$\begin{aligned}\Theta_l \triangleq& \boldsymbol{a}^T(\theta)\boldsymbol{w}_l = \sum_{m=1}^{M} w_{m,l}\exp\left\{-j\pi(m-1)\sin\theta\right\}\\ =&|\Theta_l|\exp\left\{j\angle\Theta_l\right\},\end{aligned} \tag{8}$$

where $\angle\Theta_l$ denotes the phase of the complex variable Θ_l. From (7), we can see that the value of $r_{n,l}$ at a fixed receive antenna n is dependent on the variable Θ_l. Thus, we can readily shown the following equality of

$$r_{n,l'} = \frac{\Theta_{l'}}{\Theta_l} r_{n,l} = \frac{|\Theta_{l'}|}{|\Theta_l|}\exp\{j(\angle\Theta_{l'} - \angle\Theta_l)\} r_{n,l}. \tag{9}$$

We may infer from (8) and (9) that the magnitude of $r_{n,l}$ has the RIP, if the condition $|\Theta_{l'}| = |\Theta_l|$ is met by a specifically designed beamforming matrix $\boldsymbol{W}$. A simple design of $\boldsymbol{W}$ that satisfies this condition has the following structure [15]

$$\boldsymbol{W} \triangleq \begin{bmatrix} w_{1,1} & \ldots & w_{1,\frac{L}{2}} & w^*_{M,1} & \ldots & w^*_{M,\frac{L}{2}} \\ w_{2,1} & \ldots & w_{2,\frac{L}{2}} & w^*_{M-1,1} & \ldots & w^*_{M-1,\frac{L}{2}} \\ \vdots & \ddots & \vdots & \vdots & \ddots & \vdots \\ w_{M,1} & \ldots & w_{M,\frac{L}{2}} & w^*_{1,1} & \ldots & w^*_{1,\frac{L}{2}} \end{bmatrix}, \tag{10}$$

where L is restricted to be an even number. Moreover, the conjugate transpose of $\boldsymbol{w}_{l+\frac{L}{2}}$ is the flipped version of $\boldsymbol{w}_l$ for $i = 1, \ldots, \frac{L}{2}$. In this case, it is not hard to show the following equality of

$$\angle\frac{r_{n,l'}}{r_{n,l}} = \Gamma(\theta), \quad \text{for} \quad l' = l + \frac{L}{2} \mod L, \tag{11}$$

where $\Gamma(\theta)$ denotes a fixed function of θ, which can be known as a look-up table at the reader. Based on (9) and (11), the unknown parameter θ can be obtained as

$$\theta = \Gamma^{-1}\left(\angle\frac{r_{n,l'}}{r_{n,l}}\right), \quad \text{for} \quad l' = l + \frac{L}{2} \mod L, \tag{12}$$

which can be simply found from a predefined look-up table.

On the other hand, the values of beamforming weights in $\boldsymbol{W}$ shall be chosen so that the transmit beampattern at the angles of interests is not below a certain desired levels. This is reasonable since the receiving power at the target should be higher than certain sensitivity levels. Based on (3) and (8), the transmit power distribution pattern can be expressed as

$$\begin{aligned}R_\theta \triangleq& \left\|\boldsymbol{a}^T(\theta)\boldsymbol{W}\right\|_2^2 = \sum_{l=1}^{L}\left|\boldsymbol{a}^T(\theta)\boldsymbol{w}_l\right|^2 = \sum_{l=1}^{L}|\Theta_l|^2\\ =&\sum_{l=1}^{\frac{L}{2}}|\Theta_l|^2 + \sum_{l=\frac{L}{2}+1}^{L}|\Theta_l|^2 \geq \epsilon_{\text{P}},\end{aligned} \tag{13}$$

where ϵ_{P} denotes the minimum sensitivity level required by the system. Then, since the condition $|\Theta_{l'}| = |\Theta_l|$ is met for any $l' = (l + \frac{L}{2} \mod L)$ by the structure of (10), the following equalities of

$$\sum_{l=1}^{\frac{L}{2}}|\Theta_l|^2 = \sum_{l=\frac{L}{2}+1}^{L}|\Theta_l|^2 = \frac{R_\theta}{2} \tag{14}$$

hold. Keeping in mind that the parameter θ is not known as *a priori* information at the pre-designing stage, a fair design criterion of beamforming is that the transmit power shall be uniformly distributed over all the possible spatial directions. Let us define $\{\phi_i : \phi_i \in [-\pi/2, \pi/2], i = 1, \ldots, J\}$ as a set of all the possible spatial directions to be considered. Furthermore, the radiation power across the transmit antennas is restricted to be the same, i.e., we have $\sum_{l=1}^{L}|v_{m,l}|^2 = P_{\text{Tx}}/M$ for $m = 1, \ldots, M$, where P_{Tx} is the total transmit power of the system. By using the beamforming structure of (10), we have

$$\begin{aligned}\frac{P_{\text{Tx}}}{M} =& \sum_{l=1}^{L}|w_{m,l}|^2 = \sum_{l=1}^{\frac{L}{2}}|w_{m,l}|^2 + \sum_{l=\frac{L}{2}+1}^{L}|w_{m,l}|^2\\ =&\sum_{l=1}^{\frac{L}{2}}\left(|w_{m,l}|^2 + |w_{M-m+1,l}|^2\right)\\ =&\sum_{l=1}^{\frac{L}{2}}\boldsymbol{w}_l^H\boldsymbol{\Upsilon}_m\boldsymbol{w}_l, \quad m = 1, \ldots, M,\end{aligned} \tag{15}$$

where $\boldsymbol{\Upsilon}_m$ is an $(M \times M)$-element matrix with the (m, m)th and $(M-m+1, M-m+1)$th entries being equal to ones, as well as with the remaining entries being zero-valued.

Based on the above-mentioned considerations, the beamforming weights in $\boldsymbol{W}$ can be obtained by solving the following optimization problem of

$$\begin{aligned} \min_{\boldsymbol{w}_1,\ldots,\boldsymbol{w}_{L/2}} \quad & \eta \\ \text{s. t.} \quad & \sum_{l=1}^{\frac{L}{2}} \left|\boldsymbol{a}^T(\phi_i)\boldsymbol{w}_l\right|^2 - \frac{\epsilon_{\mathrm{P}}}{2} \geq \eta, \quad i = 1, \ldots, J \\ & \eta \geq 0 \\ & \sum_{l=1}^{\frac{L}{2}} \boldsymbol{w}_l^H \boldsymbol{\Upsilon}_m \boldsymbol{w}_l = \frac{P_{\mathrm{Tx}}}{M}, \quad m = 1, \ldots, \left\lceil \frac{M}{2} \right\rceil, \end{aligned} \tag{16}$$

where η is an auxiliary variable. It can be readily shown that the problem of (16) belongs to the class of quadratically constrained quadratic programs (QCQPs) and can be solved by the semidefinite relaxation (SDR) with randomization approach [16] or the successive convex approximation as exemplified in [17], [18], the detail of which is omitted here due to the space limitation.

IV. Platoon-aided UAV Deployment and 3D Localization

A. Platoon-aided UAV Deployment

In order to obtain 3D localization information of a target, at least three UAVs are required to be deployed in different places for estimating DoA. For the sake of simplicity, in this paper, we consider the case that a platoon is consisted of a PL, two PMs, as well as three UAVs. Furthermore, the estimated DoA results are required to be reliably transmitted to the PL, so that efficient emergency supplies transportation can be implemented. In order to meet these requirements, we propose a platoon-aided UAV deployment strategy as follows.

First, we assume that each vehicle in the platoon is equipped with a single UAV. As soon as the platoon arrives at the target area, the PL sends a *Search* message to PMs and UAVs. Here, the *Search* message mainly contains two parts. The first part is the information of allocated channel and power resources for establishing communication links between the PL and each PM, namely PL-PM link for short, as well as between each vehicle and its UAV, namely PL-UAV or PM-UAV for short, as seen in Fig. 2. While, the second part contains destinations that PMs and UAVs are instructed to fulfill the tasks of DoA estimation. As soon as the *Search* message is received by PMs, they automatically drive to the predefined position and sends an *Estimation* message to their UAV. By contrast, the PL stay at the original position (i.e., (0,0,0)) and sends the *Estimation* messages to its UAV. Next, as shown in Fig. 2, UAVs fly to the instructed position to perform DoA estimation. It should be noted here that the rotary-wing UAVs are assumed to be employed, since they are capable of stay stationary in the air for providing reliable estimation results. Furthermore, each vehicle and its UAV are assumed to be in the same verticle line, in order to minimize the transmission distance of PL-UAV/PM-UAV. It should be noted here that in order to avoid interference, different frequency bands are employed for DOA estimation and information transmission. Then, DoA estimation results are transmitted to the PL via the established PL-UAV, PM-UAV, and PL-PM links. Finally, 3D localization results of the target is calculated at the PL, as shown below.

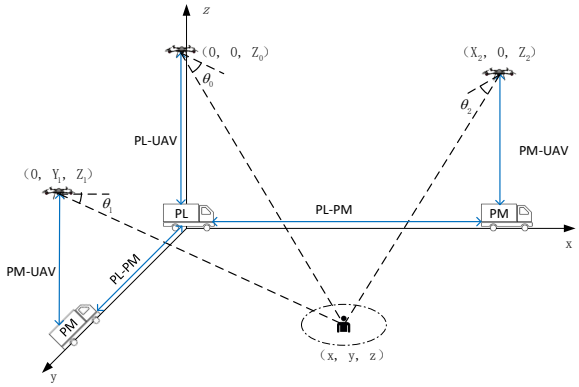

Fig. 2: Illustration of the 3D coordinate for the integrated platoon and UAV system, where three UAVs are deployed to obtain DoA information of the target located at (x, y, z).

B. 3D Localization

With the aid of the RIB design for UAVs shown in Section III, the DoA estimation can be implemented, where the DoA estimate at the uth UAV can be formulated as

$$\hat{\theta}_u = \frac{2}{LN} \sum_{n=1}^{N} \sum_{l=1}^{\frac{L}{2}} \Gamma^{-1} \left(\arctan \frac{\Im\left\{\eta_{n,l}^u\right\}}{\Re\left\{\eta_{n,l}^u\right\}} \right), \tag{17}$$

where, by definition, we have

$$\eta_{n,l}^u \triangleq \frac{y_{n,l'}^u}{y_{n,l}^u}, \quad \text{for} \quad l' = \left(l + \frac{L}{2} \mod L \right). \tag{18}$$

We can observe from (17) that our proposed system provides $LN/2$ degrees of freedom (DoFs) for the DoA estimation. Hence, a high resolution in DoA estimation is attainable, as it will be shown in Section V.

As shown in Fig. 2, the position of the PL is assumed to be the origin in the 3D coordinate. Specifically, the positions of the PMs and UAVs are assumed to be known at the PL. Specifically, we assume that the estimated DoA results are transmitted to the PL in error-free. Hence, based on Fig. 2, we can readily show the following relationship of

$$\tan\theta_0 = \frac{Z_0 - z}{\sqrt{x^2 + y^2}}, \tag{19a}$$

$$\tan\theta_1 = \frac{Z_1 - z}{\sqrt{(X_1 - x)^2 + (Y_1 - y)^2}}, \tag{19b}$$

$$\tan\theta_2 = \frac{Z_2 - z}{\sqrt{(X_2 - x)^2 + (Y_2 - y)^2}}, \tag{19c}$$

where θ_i denotes the DoA angle of the ith UAV located at (X_1, Y_1, Z_1). Finally, upon substituting the obtained DoA results into (19), the target position (x, y, z) can be readily obtained by the PL.

V. Simulation Results

In this section, simulation results are provided for investigating the performance of our integrated platoon and UAV system. The path loss is modelled by the free space model of $[57.88 + 20\log_{10}(d)]$ in dB, where d is the distance between the target and a UAV. The UAV is operated at the frequency band of 900 MHz. By contrast, the PL-PM, PL-UAV, and PM-UAV links are operated at 5.86-5.92 GHz.The noise level at each UAV is -90 dBm. The sensitivity level of the passive antenna at the target is 25 dBm. Three UAVs are deployed at the positions of (0, 0, 20 m), (0, 400 m, 20 m), (400 m, 0, 20 m), respectively. The target's position is (100 m, 100 m, -2 m), which is unknown to both platoon and UAVs.

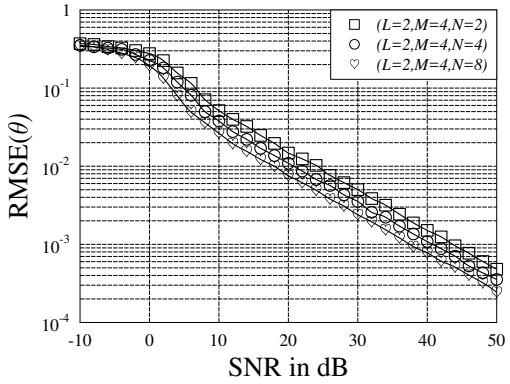

Fig. 3: RMSE(θ) versus SNR in dB for RIB-based DoA estimation in UAVs. Each UAV is equipped with $L = 2$ RF chains, $M = 4$ TAs and N RAs.

In Fig. 3, the root mean square error (RMSE) performance of the proposed RIB-based DoA estimation at UAVs is investigated. In this figure, each UAV is equipped with $L = 2$ RF chains, $M = 4$ TAs, as well as $N = 2, 4, 8$ RAs. The RIB shown in Section III is assumed to be employed at each UAV. Observe from Fig. 3 that the higher the SNR, the better the DoA estimation performence. Furthermore, the DoA estimation performance improves as the number of RAs is increased. This observation can be explained as follows. As shown in Section IV-A, the total number of received symbols conveying the DoA information at each UAV is equal to $LN/2$, yielding $LN/2$ DoF available. As the number of RAs increases, the attainable DoF is increased, hence a better estimation performance can be obtained.

Fig. 4 plots the 3D localization results obtained at the PL, which is based on the DoA estimation results from UAVs. In this figure, a single DoA test is done at each UAV with $(L = 2, M = 4, N = 2)$. Furthermore, UAVs are operated at the same SNR level of 20 dB, 30 dB, 40 dB, and 50 dB.

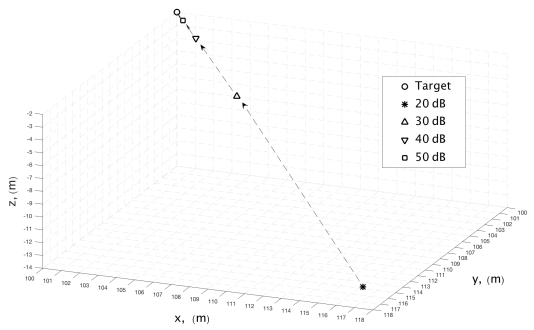

Fig. 4: 3D localization results obtained at the PL based on the DoA estimation results from UAVs, where a single DoA test is done at each UAV. Three UAVs, which are operated at the same SNR level of 20 dB, 30 dB, 40 dB, and 50 dB, are employed. Each UAV is equipped with $L = 2$ RF chains, $M = 4$ TAs and $N = 2$ RAs.

As seen in Fig. 4, the higher the SNR, the better the 3D localization results of the target. As indicated by Fig. 3, by increasing SNR, a better localization results can be obtained since more reliable DoA estimation results can be provided by UAVs.

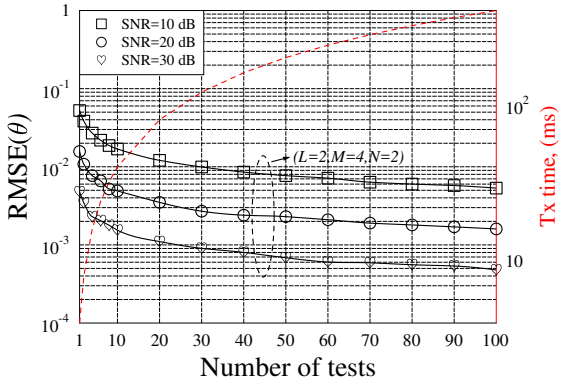

Fig. 5: RMSE(θ) (left-hand y-label) and transmission time (right-hand y-label) versus the number of samples for RIB-based DoA estimation in UAVs, where each DoA result is obtained from the collected test samples at each UAV. Specifically, the red dashed line is the corresponding transmission time. Each UAV is equipped with $L = 2$ RF chains, $M = 4$ TAs and $N = 2$ RAs.

The RMSE performance of the proposed RIB-based DoA estimation at UAVs with $(L = 2, M = 4, N = 2)$, is shown in Fig. 5. In this figure, each DoA estimation result is obtained by each UAV based on multiple DoA tests (as shown in the x-axis of Fig. 5). Moreover, three UAVs are employed with the same operating SNR level of 10 dB, 20 dB, and 30 dB. As seen in Fig. 5, the DoA estimation performance can be improved by increasing the number of tests at each UAV. However, this is achieved at the cost of higher time delay, as indicated by the red dashed line in Fig. 5.

Fig. 6 plots the 3D localization results obtained at the PL,

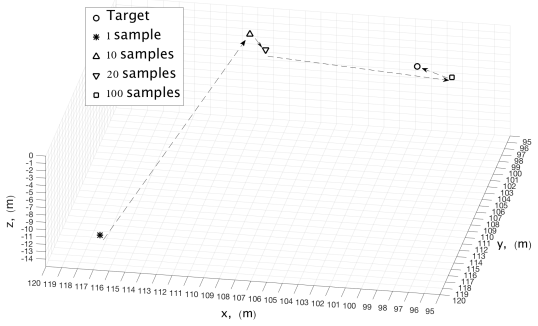

Fig. 6: 3D localization results obtained at the PL based on the DoA estimation results from UAVs, where multiple DoA tests are done at each UAV. Three UAVs operating at the same SNR level of 20 dB are employed. Each UAV is equipped with $L = 2$ RF chains, $M = 4$ TAs and $N = 2$ RAs.

where multiple tests are done at each UAV to obtain a DoA estimate. Moreover, three UAVs with $(L = 2, M = 4, N = 2)$ are employed with the same operating SNR level of 20 dB. In comparison to the localization results shown in Fig. 4, a compelling localization results can be obtained by the proposed integrated platoon and UAV system without increasing the SNR operating level of each UAV. However, as shown in Fig. 5, more testing time is required. Thus, the number of tests is required to be carefully chosen for striking the tradeoff between the DoA performance and the corresponding time delay, especially for the case of SAR.

VI. Conclusions

In this paper, 3D localization problems in SAR have been investigated, where an integrated platoon and UAV system has been proposed for fulfilling the target localization task. In order to facilitate 3D localization, a platoon-aided UAV deployment strategy has been proposed, where UAVs are deployed at different places for collecting DoA information of a target. Furthermore, a RIB scheme has been provided for MIMO UAVs to provide a simple DoA estimation. Our investigations have shown that the proposed integrated platoon and UAV system is capable of providing a good 3D localization results for SAR.

Acknowledgment

This work was supported in part by the National Natural Science Foundation of China under Grant 61571056 and 61871416, in part by the Beijing Science and Technology Nova Program under Grant xx2018083, in part by the Fundamental Research Funds for the Central Universities under Grant 2018XKJC03, and in part by the Beijing Municipal Natural Science Foundation under Grant L172010.

References

[1] D. Jia, K. Lu, J. Wang, X. Zhang, and X. Shen, "A survey on platoon-based vehicular cyber-physical systems," *IEEE Communications Surveys Tutorials*, vol. 18, no. 1, pp. 263–284, Firstquarter 2016.

[2] C. Campolo, A. Molinaro, G. Araniti, and A. O. Berthet, "Better platooning control toward autonomous driving : An LTE device-to-device communications strategy that meets ultralow latency requirements," *IEEE Vehicular Technology Magazine*, vol. 12, no. 1, pp. 30–38, March 2017.

[3] H. Peng, D. Li, Q. Ye, K. Abboud, H. Zhao, W. Zhuang, and X. Shen, "Resource allocation for cellular-based inter-vehicle communications in autonomous multiplatoons," *IEEE Transactions on Vehicular Technology*, vol. 66, no. 12, pp. 11 249–11 263, Dec 2017.

[4] K. P. Valavanis and G. J. Vachtsevanos, *Handbook of unmanned aerial vehicles*. Springer Netherlands, 2015.

[5] Y. Zeng, R. Zhang, and T. J. Lim, "Wireless communications with unmanned aerial vehicles: opportunities and challenges," *IEEE Communications Magazine*, vol. 54, no. 5, pp. 36–42, May 2016.

[6] T. Tomic, K. Schmid, P. Lutz, A. Domel, M. Kassecker, E. Mair, I. L. Grixa, F. Ruess, M. Suppa, and D. Burschka, "Toward a fully autonomous uav: Research platform for indoor and outdoor urban search and rescue," *IEEE Robotics Automation Magazine*, vol. 19, no. 3, pp. 46–56, Sep. 2012.

[7] F. Lazzari, A. Buffi, P. Nepa, and S. Lazzari, "Numerical investigation of an uwb localization technique for unmanned aerial vehicles in outdoor scenarios," *IEEE Sensors Journal*, vol. 17, no. 9, pp. 2896–2903, May 2017.

[8] Y. Shih, A. Pang, and P. Hsiu, "A doppler effect based framework for wi-fi signal tracking in search and rescue operations," *IEEE Transactions on Vehicular Technology*, vol. 67, no. 5, pp. 3924–3936, May 2018.

[9] Y. Zhang and W. Cheng, "Trajectory and power optimization for multi-uav enabled emergency wireless communications networks," in *2019 IEEE International Conference on Communications Workshops (ICC Workshops)*, May 2019, pp. 1–6.

[10] D. Fan, F. Gao, B. Ai, G. Wang, Z. Zhong, and A. Nallanathan, "Self-positioning for uav swarm via rare direction-of-arrival estimator," in *2018 IEEE Global Communications Conference (GLOBECOM)*, Dec 2018, pp. 1–6.

[11] C. Wang, J. Wang, Y. Shen, and X. Zhang, "Autonomous navigation of uavs in large-scale complex environments: A deep reinforcement learning approach," *IEEE Transactions on Vehicular Technology*, vol. 68, no. 3, pp. 2124–2136, March 2019.

[12] W. Xie, L. Wang, B. Bai, B. Peng, and Z. Feng, "An improved algorithm based on particle filter for 3D UAV target tracking," in *2019 IEEE International Conference on Communications (ICC)*, May 2019, pp. 1–6.

[13] Y. Zheng, S. Eben Li, J. Wang, D. Cao, and K. Li, "Stability and scalability of homogeneous vehicular platoon: Study on the influence of information flow topologies," *IEEE Transactions on Intelligent Transportation Systems*, vol. 17, no. 1, pp. 14–26, Jan 2016.

[14] D. Tse and P. Viswanath, *Fundamentals of wireless communication*. Cambridge University Press, 2005.

[15] A. Khabbazibasmenj, A. Hassanien, S. A. Vorobyov, and M. W. Morency, "Efficient transmit beamspace design for search-free based doa estimation in mimo radar," *IEEE Transactions on Signal Processing*, vol. 62, no. 6, pp. 1490–1500, March 2014.

[16] N. D. Sidiropoulos and T. N. D. and, "Transmit beamforming for physical-layer multicasting," *IEEE Transactions on Signal Processing*, vol. 54, no. 6, pp. 2239–2251, June 2006.

[17] H. Zhang, C. Jiang, L. Kuang, Y. Qian, and S. Guo, "Cooperative qos beamforming for multicast transmission in terrestrial-satellite networks," in *GLOBECOM 2017 - 2017 IEEE Global Communications Conference*, Dec 2017, pp. 1–6.

[18] H. Zhang, C. Jiang, J. Wang, L. Wang, Y. Ren, and L. Hanzo, "Multicast beamforming optimization in cloud-based heterogeneous terrestrial and satellite networks," *IEEE Transactions on Vehicular Technology*, vol. 69, no. 2, pp. 1766–1776, Feb 2020.